Lmtk3-KO mice display a range of behavioural abnormalities and have an impairment in GluA1 trafficking

Kristopher Montrose[1*], Shizuka Kobayashi[2], Toshiya Manabe[2] and Tadashi Yamamoto[1*]

[1]Cell Signal Unit, Okinawa Institute of Science and Technology Graduate University, Okinawa 904-0495, Japan; [2]Division of Neuronal Network, Institute of Medical Science, University of Tokyo, Tokyo 108-8639, Japan

Correspondence should be addressed to: kristopher.montrose@oist.jp or tadashi.yamamoto@oist.jp

Abstract

Accumulating evidence suggests that glutamatergic signalling and synaptic plasticity underlie one of a number of ways psychiatric disorders appear. The present study reveals a possible mechanism by which this occurs, through highlighting the importance of LMTK3, in the brain. Behavioural analysis of *Lmtk3*-KO mice revealed a number of abnormalities that have been linked to psychiatric disease such as hyper-sociability, PPI deficits and cognitive dysfunction. Treatment with clozapine suppressed these behavioural changes in *Lmtk3*-KO mice. As synaptic dysfunction is implicated in human psychiatric disease, we analysed the LTP of *Lmtk3*-KO mice and found that induction is severely impaired. Further investigation revealed abnormalities in GluA1 trafficking after AMPA stimulation in *Lmtk3*-KO neurons, along with a reduction in GluA1 expression in the post-synaptic density. Therefore, we hypothesize that LMTK3 is an important factor involved in the trafficking of GluA1 during LTP, and that disruption of this pathway contributes to the appearance of behaviour associated with human psychiatric disease in mice.

Introduction

LMTK3 is a member of the Lemur tyrosine kinase (LMTK) family of serine/threonine protein kinases, expressed predominantly in the brain. The other family members, LMTK1 and LMTK2, are reportedly involved in regulating endocytosis. For example, LMTK1 regulates the movement of recycling endosomes via Rab11A and influences dendrite development and axon outgrowth (Takano et al., 2012; Takano et al., 2014). Whereas LMTK2 is critical for transitioning early endosomes to recycling endosomes through binding of the motor protein, Myosin VI (Inoue et al., 2008). Despite its high expression in the brain, little is known about the physiological role of LMTK3. We previously found that *Lmtk3*-KO mice exhibit hyperactivity and reduced anxiety with slightly increased amounts of intracellular NMDA receptors (Inoue et al., 2014). We hypothesized that the abnormal behaviour of *Lmtk3*-KO mice could be linked to changes in synaptic function. A number of psychiatric diseases, most prominently schizophrenia and bipolar disease are thought to be synaptopathies, a disease of the brain or nervous system related to dysfunctional synapses. This is due to patients with these particular psychiatric diseases bearing mutations in a number of genes associated with synaptic development and function (Du et al., 2011; Forero et al., 2009; Stephan et al., 2006). Symptoms of these diseases often overlap, and recent reports have shown that this maybe a consequence of shared genetic risk factors (Doherty & Owen, 2014; Gandal, 2018). Increasing evidence has led to the hypothesis that dysfunctional glutamatergic synaptic transmission is a factor in many brain related disorders including schizophrenia and mood disorders (Jun et al., 2014; Konradi & Heckers, 2003; Rubio et al., 2012). AMPA (α-amino-3-hydroxy-5-methyl-4-isoxazolepropionic acid)-type glutamate receptors (AMPARs) mediate fast excitatory neurotransmission, and the internalization or re-insertion of AMPAR subunits at post-synaptic sites regulates long-term potentiation (LTP) or long-term depression (LTD) (Henley & Wilkinson, 2013; Huganir & Nicoll, 2013). A number of reports have revealed abnormal expression of AMPARs in post-mortem brain samples from patients diagnosed with schizophrenia and bipolar disease suggesting an important pathological role for these glutamate receptors (Corti et al., 2011; Heckers & Konradi, 2002; Meador-Woodruff et al., 2001). In this study, we further analysed the behaviour of *Lmtk3*-KO mice and discovered that they exhibited changes in behaviour and memory commonly associated with psychiatric disease. Treatment with clozapine, an antipsychotic primarily used to treat schizophrenia patients, but which is also effective for bipolar disease (Fehr et al., 2005; Frye et al., 1998) and suggested for ASD patients (Beherec

et al., 2011; Rotharmel et al., 2018), attenuated the abnormal behaviour of *Lmtk3*-KO mice. As synaptic dysfunction is relevant to the behaviour displayed by *Lmtk3*-KO mice, we conducted electrophysiological studies and discovered that LTP is disrupted in *Lmtk3*-KO mice. Further investigation revealed that trafficking of AMPARs, which can directly influence LTP, is altered by the loss of LMTK3. Cultured neurons derived from *Lmtk3*-KO mice display abnormal surface and intracellular expression of the AMPAR subunit, GluA1, after stimulation with the excitatory neurotransmitter, AMPA. Analysis of forebrain tissue revealed a reduction of GluA1 expression in the post-synaptic density of *Lmtk3*-KO mice. We propose that LMTK3 plays a role in the trafficking of GluA1 during synaptic plasticity, particularly LTP, which is required for regulating behaviour and cognitive function.

Materials and Methods

Animals

Lmtk3-KO mice have a C57BL/6J genetic background. The generation and validation of *Lmtk3* KO mice is described by Inoue et al 2014. Mice were housed at a constant temperature (23±1°C) and kept under a 12-h light/dark cycle.

Behavioural analysis

Behavioural experiments were performed with wild type (WT) and knockout (*Lmtk3*$^{-/-}$) male littermates (8-12 weeks old). All recordings were blind with regard to genotype. For clozapine treatments, littermates were randomly distributed to control and treatment groups. Clozapine (Sigma) was dissolved in DMSO:saline (1:6), and mice were IP injected with a dose of 2 mg/kg. Control mice were injected with DMSO:saline at equivalent volumes. Behavioural assays were conducted 30 min after injection. All animal experiments were performed following the guidelines for animal use issued by the Animal Ethics Committee, Okinawa Institute of Science and Technology.

Three-chamber social interaction test

Mice were placed in a three-chamber box (61 cm width x 40 cm length x 22 cm height) with removable partitions separating the box into left, right, and centre chambers. The left and right chambers contained small cages able to hold single mice. Age- and gender-matched C57BL/6J mice (JapanSLC) were used as novel partners. First, test mice were habituated in

the chamber for 10 min. Next, a novel mouse was placed in one of the cages and test mice were allowed to explore the chambers for 10 min. Immediately after, the social novelty trial was conducted for a further 10 min, with a new mouse being placed in the second empty cage. Total movement and time spent in close interaction with mice in cages were recorded and automatically measured with TimeSCI software (O'hara & Co).

Novel object recognition test

The novel object recognition apparatus consisted of an open-field box illuminated at 100 lux. During the training session, mice were placed in the apparatus in the presence of two identical objects and allowed to explore for 10 min. After a retention interval of 24 h, mice were again placed inside the apparatus for 10 min, with one of the previous objects replaced with a novel object. The duration of time mice spent interacting with each object was recorded and measured with Image SCI software (O'hara & Co).

Pre-pulse inhibition of the acoustic startle response

Mice were restrained in a Plexiglas chamber (O'hara & Co)and acclimated to experimental conditions for 2 min. The startle response was recorded for 200 ms after onset of the stimulus. The peak startle amplitude during the 200 ms sampling window was recorded as a measure of the startle response. Background noise level was at 70 dB. A test session consisted of a habituation block where a startle stimulus (120 dB) was presented four times with random inter-trial times (10-20s). The second block, conducted immediately after the first, consisted of 4 prepulse trial types, where a pre-pulse sound (75, 80 or 85 dB) or no prepulse was presented 100 ms before the startle stimulus (120 dB). Trials were pseudorandomized and presented 8 times each, with inter-trial intervals of (10-20s). The following formula was used to calculate the percentage of pre-pulse inhibition of the startle response, 100-(100 x (startle response after pre-pulse/startle response alone).

Morris water maze

The Morris water maze test was performed in a circular pool (30 cm height x 100 cm in diameter), filled with water at a temperature of 22-24°C, made opaque with non-toxic white paint. The pool was divided into four quadrants and a white platform was placed in the middle of one of the quadrants, 1 cm below the water surface. One day prior to testing, mice were allowed to swim for 60 s in the pool with the platform visible with a flag marker. In the hidden platform test, three trials per day with inter-trial intervals of 30 min were conducted

for six consecutive days. The latency to reach the platform for each trial was recorded with a cut-off time of 60 s. Twenty-four hours after the final training day, the platform was removed and the probe test was conducted for 60 s. The time spent in each quadrant, and number of crossings of the target site was recorded. In the visible platform test, three trials per day with inter-trial intervals of 30 min were conducted for three consecutive days. The platform was clearly marked with a flag in each trial. The latency to find the platform was recorded with a cut-off time of 60 sec. All recordings and measurements were conducted using Time MWM software (O'hara & Co).

Eight-arm radial maze

The eight-arm radial maze consisted of a central chamber and eight arms with a door at the entrance of each arm, which opened and shut automatically, according to the movement of mice. Mice used in this test had undergone restriction feeding until ~20% of body weight was lost. The day before testing, mice were habituated to the maze by being allowed to roam the chambers for 15 min. During the testing phase, a food pellet was placed at the end of each of the eight arms, and mice were allowed to explore for 15 min. After four food pellets were consumed, a delay was implemented with mice restricted to the central chamber for 1 min. The testing phase was conducted once a day for six consecutive days. Latency to consume all food pellets, number of entries into each arm and number of entries before repeat entry was automatically recorded and measured using Time ERM software (O'hara & Co).

Y-maze

Mice were placed in one arm of a three arm maze, illuminated at 50 lux, and the entry sequence into each arm and number of arm entries were recorded using Time YM (O'hara & Co) software for 10 min. The percentage of triads in which all arms were represented was recorded as an alternation. The alternation score (%) was calculated using the following equation: number of alternations/total arm entries -2 x100.

Open-field test

Mice were placed in the centre of an open-field apparatus (50 cm width x 50 cm depth x 33.3 cm height) illuminated at 150 lux and allowed to move freely for 15 min. The total distance travelled, rearing activity, and time spent in specific areas of the open field were recorded and analysed with Time OFCR software (O'hara & Co).

Elevated plus maze test

The elevated plus maze consists of two open arms and two closed arms (25 cm length x 5 cm width) extending from a central area (5 x 5 cm) and is elevated 50 cm from the ground. Mice were placed in the central area and allowed to move freely for 10 min. The number of entries into open or closed arms and time spent in each arm was recorded and analysed using Time EPC software (O'hara & Co).

Light/dark transition test

The light-dark box consisted of two compartments: a white polyvinylchloride chamber illuminated at 500 lux and a black polyvinylchloride chamber with no illumination (19 x 19 x 19 cm). The two boxes were separated by a vertical sliding door that remained open. Mice were placed in the dark chamber and allowed to explore freely for 15 min. The amount of time spent in each chamber and the number of transitions between chambers were recorded and analysed using Time LD software (O'hara & Co.).

Contextual and auditory fear conditioning tests

Fear conditioning was conducted in a small conditioning chamber within a sound attenuating chest (CL-M3; O'hara & Co.). On day 1, mice were placed in the conditioning chamber for 170 s and then presented with a 65dB/10kHz tone for 10 s followed by a foot shock (2s/0.35 mA). The mice were returned to their home cages after 1 min. On day 2, mice were placed in the conditioning chamber for 6 min. On day 3, the mice were placed in a novel chamber for 3 min and then presented with a tone for 3 min. Freezing responses were recorded during each test and analysed using Image FZC 2.22sr2 software (O'hara & Co.).

Antibodies

To generate polyclonal antibodies against LMTK3, a fragment of human LMTK3 (aa 1000–1100) was used as an immunogen. Antibodies were purified by affinity chromatography from sera of immunized rabbits. Commercially available antibodies used are as follows: mouse anti-GluR1 N-terminal (Millipore); rabbit anti-phospho-GluR1 (Ser845), rabbit anti-GluR2, rabbit anti-beta actin (Cell signalling); mouse anti-synaptophysin (Sigma); mouse anti-PSD-95 (Affinity Bioreagents); goat anti-mouse-Alexa488 and anti-mouse-Alexa555 (Invitrogen).

Cell culture and 'antibody feeding' immunocytochemistry

Cortical neurons were prepared from 16-18 day mouse embryos, and cultured according to a standard protocol (Inoue et al., 2014). Cultured neurons grown on glass-bottomed dishes (MatTek) were fixed with 4% PFA in PBS and permeabilized with 0.2% Triton X-100 in PBS before labelling with fluorescent secondary antibodies. The 'antibody feeding' method was conducted according to published methods (Lin et al., 2000). Images were acquired using a scanning confocal microscope (Leica TCS-SP8).

Surface biotinylation of cultured neurons

Primary cortical and hippocampal neuronal cultures at DIV14 were treated with 100 µm AMPA (Santa Cruz) for various lengths of time, and then immediately placed on ice. Surface proteins were biotinylated with 1 mg/mL sulfo-NHS-SS cleavable biotin (Pierce) for 20 min at 4°C. Cells were washed with PBS supplemented with 1 mM $MgCl_2$ and 0.1 mM $CaCl_2$ (PBS/MC) and cells were then lysed with lysis buffer (120 mM NaCl, 50 mM Tris, 5 mM EDTA, 1% NP40, 0.1% sodium deoxycholate, 1mM Na_3VO_4 and protease inhibitor cocktail (Nacalai Tesque). Biotinylated proteins were precipitated with Neutravidin resins (Pierce). To collect internalized proteins, neurons were biotinylated by the same method as above, then subjected to treatment with AMPA and returned to 37°C for described times. Neurons were then rapidly cooled to 4°C, and washed with PBS/MC. Biotinylated surface proteins were cleaved with cleavage buffer (50 mM glutathione, 75 mM NaCl, 10 mM EDTA, 1% BSA and 0.075 N NaOH), and biotinylated proteins precipitated.

Biochemical fractionation

Mouse brains were homogenized in ice-cold HEPES buffer (0.32M sucrose, 10 mM HEPES pH 7.4, 2 mM EDTA and protease inhibitors) using a Dounce homogenizer. The homogenate was centrifuged at 1000 x g, and supernatant was removed and re-centrifuged at 12,500 x g to obtain a crude synaptosomal fraction (P2). The P2 fraction was lysed hypo-osmotically and centrifuged at 25,000 x g to yield a synaptosomal membrane fraction. The post-synaptic density fraction (PSD) was obtained by treating the synaptosomal membrane fraction with HEPES buffer containing 1% Triton X-100 and centrifugation at 32,000 x g.

Electrophysiological analysis

Standard procedures and solutions were used to prepare hippocampal slices (400 µM thick) from 10–17 week-old wild-type and *Lmtk3*-KO mice (Bongsebandhu-phubhakdi & Manabe,

2007). Synaptic responses were recorded at 25.0 ± 0.5°C with extracellular field-potential recordings in the stratum radiatum of the CA1 region. External solution contained (in mM): 119 NaCl, 2.5 KCl, 1.3 $MgSO_4$, 2.5 $CaCl_2$, 1.0 NaH_2PO_4, 26.2 $NaHCO_3$, 11 glucose and 0.1 picrotoxin, a $GABA_A$-receptor antagonist (Sigma). To evoke synaptic responses, Schaffer collateral/commissural fibers were stimulated at 0.1 Hz with a bipolar tungsten electrode. Stimulus strength was adjusted to evoke EPSPs with a slope value of 0.10–0.15 mV/ms. A recording glass electrode was filled with 3 M NaCl. LTP was induced by 10 trains of theta-burst stimulation (TBS) at 10 sec intervals. One train of TBS consisted of 5 bursts at 5 Hz, and each burst comprised 4 pulses at 100 Hz. An Axopatch-1D amplifier (Molecular Devices, Union City, CA, USA) was used to record synaptic responses. Data were filtered at 1 kHz, digitized at 10 kHz with Digidata 1440A (Molecular Devices) and analyzed on-line and off-line using pClamp software (Molecular Devices).

Statistical analysis

All data are expressed as means ± SEMs. We used Student's *t*-test for biochemical analysis. To analyse behavioural data, we used two-way/two-way repeated-measures ANOVA and Student's *t*-test as indicated. Significant ANOVAs were followed up with Bonferroni's *post-hoc* test. Values with $p < 0.05$ were considered significant.

Results

Lmtk3-KO mice exhibit altered behavioural patterns

Having previously observed that *Lmtk3*-KO mice exhibit hyperactivity and reduced anxiety, we analysed whether other behaviours commonly found in mouse models of psychiatric disease are also exhibited. Social behaviour was tested using a three-chamber social interaction test. During habituation, there was no preference for either of the empty cages present in the left and right chambers ($F_{(1,36)} = 2.035$, $p = 0.1624$ for genotype effect and $F_{(1,36)} = 0.2001$, $p = 0.6573$ for cage effect) (Fig. 1A). When a stranger mouse was placed in one of the empty cages, *Lmtk3*-KO mice interacted with the stranger mouse longer than WT ($F_{(1,36)} = 4.34$, $p < 0.043$ for genotype effect; *post-hoc* analysis, $p = 0.0016$ for interaction time with stranger mouse) (Fig. 1B). During the social novelty test, *Lmtk3*-KO mice spent equal time interacting with stranger and familiar mice, indicating impaired social memory and novelty ($F_{(1,36)} = 17.26$, $p < .0002$ for genotype x test mouse interaction; *post-hoc* analysis, $p < 0.0001$ for interaction time of WT mice) (Fig. 1C). To confirm loss of novelty,

we performed the novel object recognition test and found that both genotypes spent equal time between two novel objects ($F_{(1,28)} = 0.1101$, $p = 0.74$ for genotype effect; $F_{(1,28)} = 0.0994$, $p = 0.75$ for genotype x object interaction) (Fig. 1D). When one object was replaced with a novel object, WT mice interacted longer with the novel object ($F_{(1,28)} = 8.681$, $p < 0.0064$ for genotype effect; $F_{(1,28)} = 8.265$, $p < 0.05$ for genotype x object interaction; *post-hoc* analysis, $p = 0.011$ for interaction time of WT mice) (Fig. 1E). The prepulse inhibition (PPI) of *Lmtk3*-KO mice was previously analysed during the acoustic startle response test, and results showed only a slight reduction (Inoue et al., 2014). Here we repeated the PPI test independently from the acoustic startle response test, as a number of reports have shown that the baseline stimulus can effect PPI, and exposure to different baseline stimuli which occurs during the acoustic startle response test can lead to inaccurate results (Sandner & Canal, 2007; Shoji & Miyakawa, 2018). What we found was that the PPI response in *Lmtk3*-KO mice is significantly attenuated for three different prepulse intensities ($F_{(1,42)} = 24.20$, $p < 0.0001$ for genotype effect; *post-hoc* analysis, $p = 0.0399$ for 75dB, $p = 0.0019$ for 80 dB, $p = 0.014$ for 85dB) (Fig. 1F). There was no significant difference in the acoustic startle response between genotypes to the single baseline stimulus (120 dB) used, as previously shown ($F_{(1,14)} = 0.04$, $p = 0.844$ for genotype effect) (Fig. 1G).

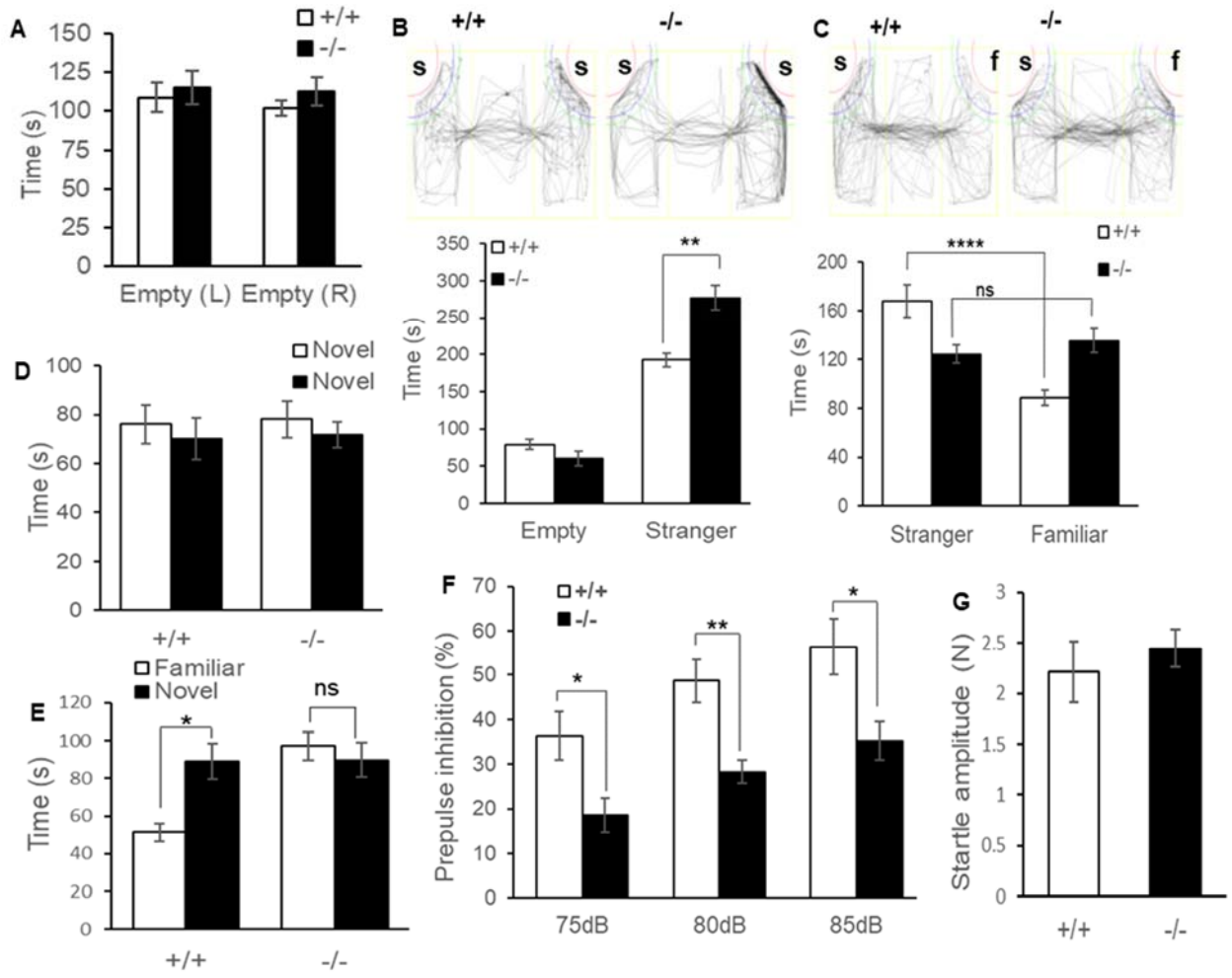

Figure 1. *Lmtk3*-KO mice exhibit changes in sociability, novel recognition and PPI

(A-C) Three-chamber social interaction test. (WT, $n = 12$; KO, $n = 12$). **P < 0.01, ****P < 0.0001, (ns) not significant; two-way ANOVA followed by Bonferroni's test. (A) During habituation, there is no preference for a particular cage by either genotype (B) *Lmtk3*-KO mice interact longer with stranger mice than WT after 10 min. (C) *Lmtk3*-KO show no preference for stranger or familiar mice after 10 min. (D-E) Novel object recognition test. (WT, $n = 8$; KO, $n = 8$). *P < 0.05, (ns) not significant; two-way ANOVA followed by Bonferroni's test. (D) No differences were observed between genotypes in interaction time with two novel objects. (E) WT spend more time interacting with a novel object, whereas *Lmtk3*-KO exhibit no preference. (F-G) Pre-pulse inhibition test. (WT, $n = 8$; KO, $n = 8$). **P < 0.01, *P < 0.05; two-way ANOVA followed by Bonferroni's test. (F) *Lmtk3*-KO exhibited impaired pre-pulse inhibition (PPI) at three pre-pulse intensities. (G) No difference is found in the startle response to the base stimuli of 120 dB by either genotype. All values represent means ± SEM.

Lmtk3-KO mice display cognitive dysfunction

Next, we assessed the cognitive function of *Lmtk3*-KO mice. During the Morris water maze, *Lmtk3*-KO mice failed to find the hidden platform, even after six training days ($F_{(1,14)} = 9.944$, $p = 0.0070$ for genotype effect; $F_{(5,70)} = 2.829$, $p = 0.0220$ for genotype x day) (Fig. 2A). In the probe test conducted 24 hrs after the final training day, *Lmtk3*-KO mice performed poorly, with fewer crossings of the trained platform position (*t*-test $p = 0.030$) and less time spent in the trained quadrant compared to WT mice (*t*-test $p = 0.024$) (Fig. 2B, 2C). No difference between WT and *Lmtk3*-KO mice in the visible water maze test was observed (Fig. 2D). The Y-maze test revealed *Lmtk3*-KO mice have a deficit in short-term working memory, with *Lmtk3*-KO mice producing significantly fewer spontaneous alternations (*t*-test $p = 0.004$) (Fig. 2E). *Lmtk3*-KO mice also exhibited a lack of learning and memory in the eight arm radial maze test, as there were more errors made by *Lmtk3*-KO mice over 7 days of training ($F_{(1,14)} = 5.137$, $p = 0.039$ for genotype effect; $F_{(6,84)} = 2.515$, $p = 0.0275$ for genotype x day) (Fig. 4F). Working memory span capacity, which was measured as the number of arms entered before a repeat entry, was also lower in *Lmtk3*-KO mice ($F_{(1,14)} = 12.22$, $p < 0.001$ for genotype effect; $F_{(6,84)} = 4.112$, $p = 0.0011$ for genotype x day) (Fig. 2G).

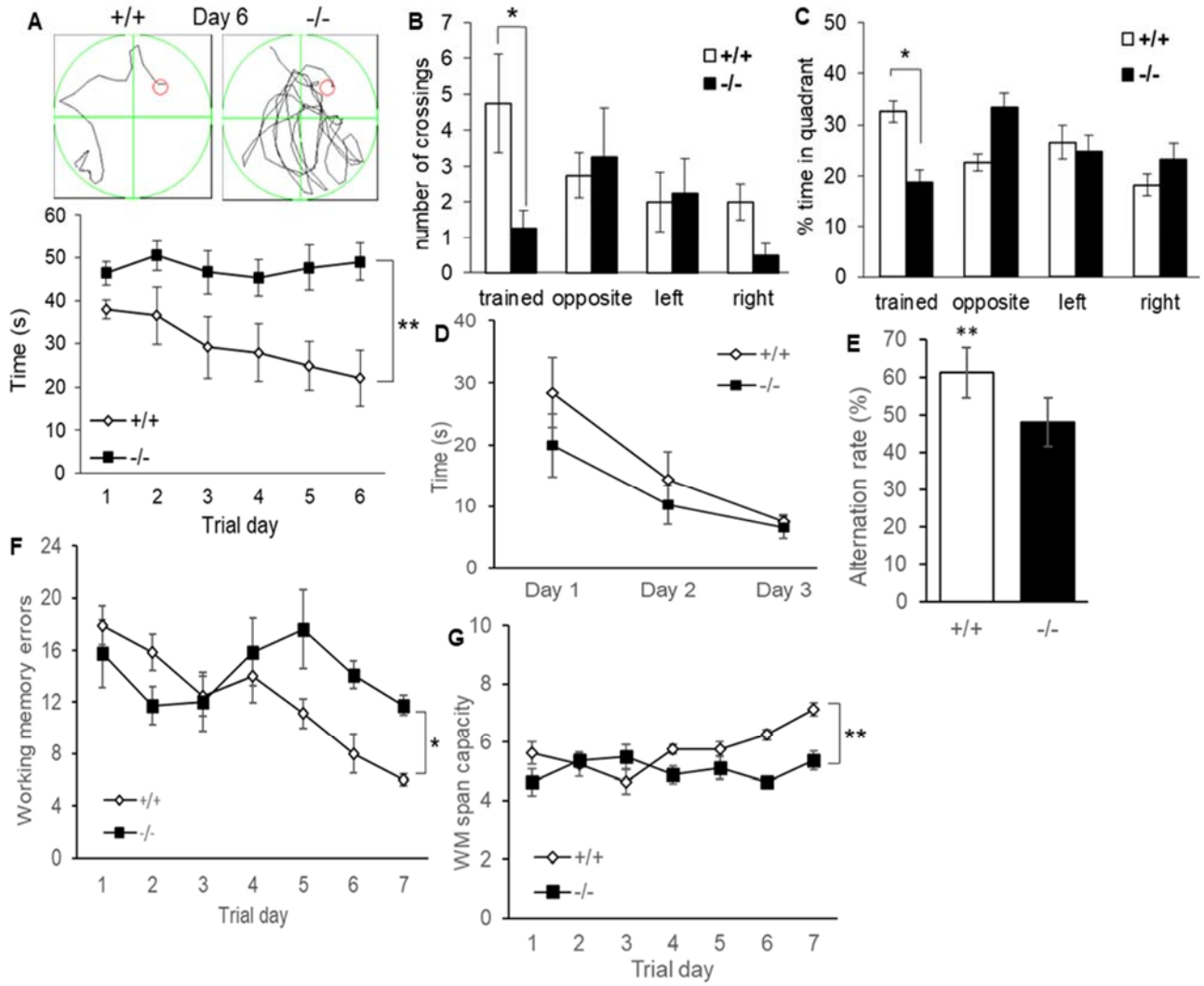

Figure 2. *Lmtk3*-KO mice exhibit cognitive dysfunction

(A-C) Morris water maze. (WT, $n = 8$; KO, $n = 8$). **P < 0.01, *P < 0.05; two-way repeated measures ANOVA (Fig. A) and un-paired two tailed *t*-test (Fig. B, C). (A) *Lmtk3*-KO show no improvement in latency during training (results shown are the means of three trials). (B) The probe test conducted 24 h after final training day shows fewer crossings of the trained platform position by *Lmtk3*-KO. (C) Less time is spent in the trained quadrant by *Lmtk3*-KO. (D) Visible water maze. (WT, $n = 8$; KO, $n = 8$). There is no difference in latency to locate a visible platform between WT and *Lmtk3*-KO mice. (E) Y-maze. (WT, $n = 10$; KO, $n = 10$). **P < 0.01; un-paired two tailed *t*-test. *Lmtk3*-KO produce fewer spontaneous alternations in 10 min. (F-G) Eight-arm radial maze. (WT, $n = 8$; KO, $n = 8$). **P < 0.01, *P < 0.05; two-way repeated measures ANOVA. (F) *Lmtk3*-KO are more prone to committing working memory errors than WT over 7 training days. (G) *Lmtk3*-KO have a lower working memory span. All values represent means ± SEM

Clozapine suppresses the behavioural changes of *Lmtk3*-KO mice

A number of psychiatric mouse models display behaviour similar to that of *Lmtk3*-KO mice, primarily models for schizophrenia and bipolar disorder (Cosgrove et al., 2016; Jones et al., 2011; Leo & Gainetdinov, 2013). Human patients and animal models of these diseases have been known to respond to treatment with antipsychotics, therefore we treated *Lmtk3*-KO mice with clozapine which is prescribed to treat a range of psychiatric diseases (Fehr et al., 2005; Li et al., 2015; Remington et al., 2016; Siskind et al., 2016). Mice were treated with IP injections of clozapine (2 mg/kg) and behavioural testing was conducted 30 min later. The locomotor activity of *Lmtk3*-KO mice compared to vehicle-treated *Lmtk3*-KO mice during the open field test was lower ($F_{(1,28)} = 2.731$, $p < 0.0001$ for genotype effect; $F_{(1,28)} = 36.61$, $p < 0.0001$ for drug effect; $F_{(1,28)} = 6.673$, $p = 0.015$ for drug x genotype; *post-hoc* analysis, $p = < 0.0001$ for KO vehicle vs. KO clozapine) (Fig. 3A). Hyperactivity was not fully suppressed in *Lmtk3*-KO treated mice, which could be due to the drug dose required to completely block hyperactivity being higher than what was administered in this study (McOmish et al., 2012). We were unable to increase the dosage of clozapine as initial trials revealed higher doses led to extreme sedation in *Lmtk3*-KO mice. Time spent in the centre region by *Lmtk3*-KO mice was similar to that of WT after treatment ($F_{(1,28)} = 10.84$, $p < 0.0027$ for genotype effect; $F_{(1,28)} = 3.057$, $p = 0.0913$ for drug effect; $F_{(1,28)} = 12.93$, $p = 0.0012$ for drug x genotype; *post-hoc* analysis, $p = 0.0002$ for WT vs. KO vehicle, $p = 0.0045$ for KO vehicle vs. KO clozapine), as *Lmtk3*-KO mice remained active only around the periphery of the open field (Fig. 3B). The rearing number of *Lmtk3*-KO mice was reduced, indicating a recovery from the anxiolytic effect of LMTK3 depletion ($F_{(1,28)} = 22.66$, $p < 0.0001$ for genotype effect; $F_{(1,28)} = 11.01$, $p = 0.0025$ for drug effect; $F_{(1,28)} = 9.24$, $p = 0.0047$ for drug x genotype; *post-hoc* analysis, $p < 0.0001$ for WT vs. KO vehicle, $p = 0.006$ for KO vehicle vs. KO clozapine) (Fig 3C). This was also evident in the elevated plus maze, where clozapine treatment led to *Lmtk3*-KO mice spending less time in the open arms compared to vehicle treated mice ($F_{(1,28)} = 73.03$, $p < 0.0001$ for genotype effect; $F_{(1,28)} = 63.43$, $p < 0.0001$ for drug effect; $F_{(1,28)} = 26.41$, $p < 0.0001$ for drug x genotype; *post-hoc* analysis, $p < 0.0001$ for WT vs. KO vehicle, $p < 0.0001$ for KO vehicle vs. KO clozapine) (Fig. 3D). Treated *Lmtk3*-KO mice spent less time in the light chamber during the light-dark transition test ($F_{(1,28)} = 10.54$, $p = 0.0030$ for genotype effect; $F_{(1,28)} = 6.662$, $p = 0.0154$ for drug effect; $F_{(1,28)} = 4.321$, $p = 0.0469$ for drug x genotype; *post-hoc* analysis, $p = 0.0047$ for WT vs. KO vehicle, $p = 0.0160$ for KO vehicle vs. KO clozapine) (Fig. 3E). Clozapine has notable success in treating PPI deficits (Gray et

al., 2009; Swerdlow & Geyer, 1993), therefore we also tested whether the PPI of *Lmtk3*-KO mice is recovered after treatment. Clozapine effectively reversed the deficits in PPI exhibited by *Lmtk3*-KO mice ($F_{(1,84)} = 68.47$, $p < 0.0001$ for genotype effect; $F_{(1,84)} = 5.73$, $p = 0.018$ for drug effect; $F_{(1,168)} = 9.56$, $p = 0.0027$ for drug x genotype; *post-hoc* analysis of KO vehicle vs. KO clozapine, $p = 0.04$ for 75dB,($p = 0.031$ for 80 dB, $p = 0.0221$ for 85dB) (Fig. 3F). There was no change in the sociability of *Lmtk3*-KO mice after clozapine treatment ($F_{(1,28)} = 16.08$, $p = 0.0004$ for genotype effect, $F_{(1,28)} = 3.8$, $p = 0.0613$ for drug effect, $F_{(1, 28)} = 0.05231$, $p = 0.8207$ for drug x genotype) (Fig. 3G). The deficit in social novelty seen in *Lmtk3*-KO mice also remained after treatment ($F_{(1,56)} = 0.8147$, $p = 0.3706$ for genotype effect, $F_{(1,56)} = 0.3708$, $p = 0.8196$ for drug effect, $F_{(1,56)} = 2.361$, $p = 0.811$ for drug x genotype) (Fig. 3H). This may be due to the ability of clozapine to increase social activity (Becker & Grecksch, 2003; Qiao et al., 2001), rather than attenuate.

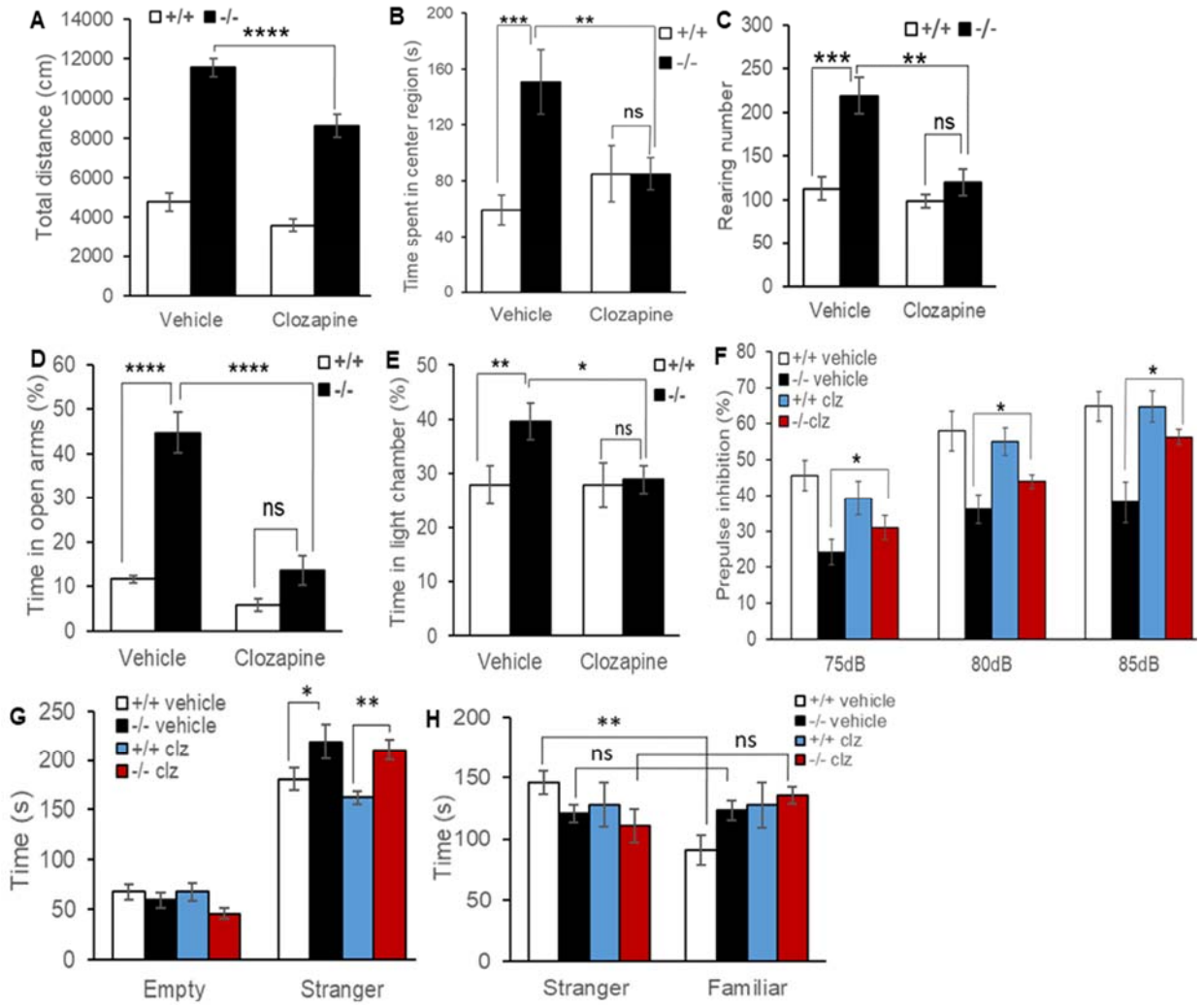

Figure 3. Clozapine suppresses the abnormal behaviour of *Lmtk3*-KO mice

(A-C) Open field test (WT, *n* = 8; KO, *n* = 8). ****P < 0.0001, ***P < 0.001, **P < 0.01, (ns) not significant; two-way ANOVA followed by Bonferroni's test. (A) Clozapine reduces the locomotor activity of *Lmtk3*-KO compared to un-treated *Lmtk3*-KO. (B) Time spent within the centre region of the open field is reduced in *Lmtk3*-KO after clozapine treatment. (C) Less rearing occurs in clozapine-treated *Lmtk3*-KO vs. vehicle treated *Lmtk3*-KO. (D) Elevated plus maze (WT, *n* = 8; KO, *n* = 8). ****P < 0.0001, (ns) not significant; two-way ANOVA followed by Bonferroni's test. Treated *Lmtk3*-KO spend less time in the open arms compared to vehicle treated mice. (E) Light-dark transition test (WT, *n* = 8; KO, *n* = 8). **P < 0.01, *P < 0.05, (ns) not significant; two-way ANOVA. Treated *Lmtk3*-KO mice spend less time in the light chamber of a light/dark box compared to vehicle treated. (F) Pre-pulse inhibition test. (WT, *n* = 8; KO, *n* = 8). *P < 0.05; repeated measures two-way ANOVA. Treated *Lmtk3*-KO display higher pre-pulse inhibition as compared to vehicle treated *Lmtk3*-

KO.(G-H) Three-chamber social interaction test (WT, $n = 8$; KO, $n = 8$). **P < 0.01, *P < 0.05, (ns) not significant; two-way ANOVA followed by Bonferroni's test. (G) *Lmtk3*-KO mice remain hyper-sociable after clozapine treatment. (H) Clozapine treated *Lmtk3*-KO mice still exhibit social novelty deficits.

Clozapine improves the memory and learning of *Lmtk3*-KO mice

During the Morris water maze, treatment with clozapine 30 min prior to each training session improved the performance of *Lmtk3*-KO mice compared to untreated mice ($F_{(1,168)} = 25.26$, $p < 0.0001$ for genotype effect; $F_{(1,168)} = 20.15$, $p < 0.0001$ for drug x genotype) (Fig. 4A). Analysis of the probe test revealed a difference in the number of crossings of the trained quadrant by *Lmtk3*-KO mice after treatment, with a significant drug x genotype interaction ($F_{(1,28)} = 29.2$, $p < 0.0001$), though no significant values were found for genotype ($F_{(1,28)} = 0.354$, $p = 0.5562$) or drug effect ($F_{(1,28)} = 0.58$, $p = 0.452$) (Fig. 4B). However, *post-hoc* analysis of the probe test revealed a significant difference between KO vehicle vs. KO clozapine ($p = 0.0245$). The same applied to time spent within the trained quadrant ($F_{(1,28)} = 5.6$, $p = 0.025$ for drug x genotype; $F_{(1,28)} = 1.2$, $p = 0.2702$ for genotype effect; $F_{(1,28)} = 0.06$, $p = 0.799$ for drug effect, *post-hoc* analysis, $p = 0.045$ for KO vehicle vs. KO clozapine) (Fig. 4C). We did find that clozapine treatment showed a tendency toward some adverse effects during the probe test but statistical analysis revealed this was not significant (WT vehicle vs. WT clozapine ($p = 0.181$) for crossings of trained quadrant; WT vehicle vs. WT clozapine ($p = 0.772$) for time spent in trained quadrant). *Lmtk3*-KO mice exhibit impaired fear memory, but in the contextual and fear conditioning test, clozapine-treated mice exhibited higher levels of freezing compared to vehicle-treated mice in response to auditory cues ($F_{(1,168)} = 64.63$, $p = 0.0001$; for genotype effect; $F_{(1,168)} = 10.94$, $p < 0.0012$; for drug effect; $F_{(1,168)} = 3.076$, $p = 0.08$ for drug x genotype) (Fig. 4D). This was also the case in response to contextual cues ($F_{(1,168)} = 12.67$, $p = 0.0005$ for genotype effect; $F_{(1,168)} = 29.2$, $p < 0.0001$ for drug effect; $F_{(1,168)} = 12.31$, $p = 0.0006$ for drug x genotype) (Fig. 4E).

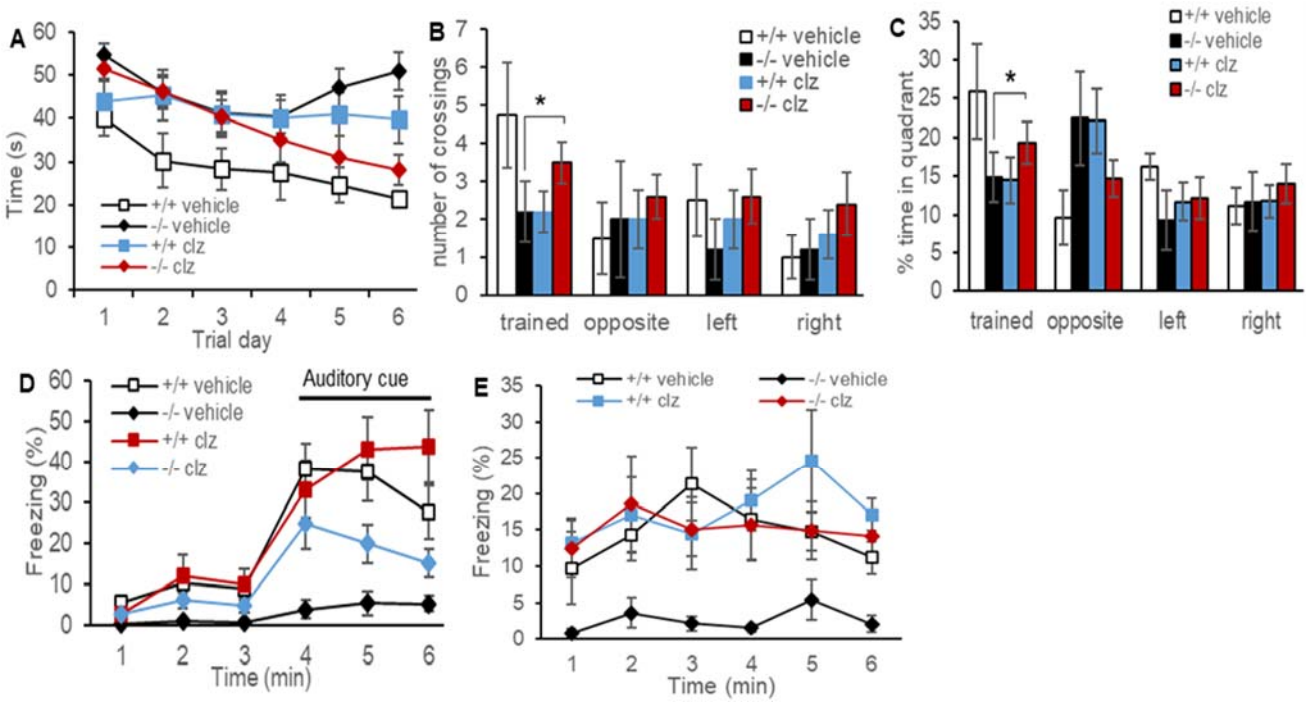

Figure 4. Clozapine improves the memory and learning of *Lmtk3*-KO mice

(A-C) Morris water maze. (WT, *n* = 8; KO, *n* = 8). *P < 0.05; repeated measures two-way ANOVA (Fig. A) and two-way ANOVA followed by Bonferroni's test (Fig. B, C). (A) Clozapine improves latency to find the hidden platform by *Lmtk3*-KO. (B) Increased number of crossings of the trained quadrant during the probe test by treated *Lmtk3*-KO compared to vehicle treated KO. (C) Longer time spent within the trained quadrant by treated *Lmtk3*-KO compared to vehicle treated KO. (D-E) Auditory and contextual fear conditioning test. (WT, *n* = 8; KO, *n* = 8), repeated measures two-way ANOVA. (D) Clozapine treatment increases the freezing response to auditory cues of *Lmtk3*-KO in comparison to un-treated KO mice. (E) Clozapine increases the freezing response to contextual cues by *Lmtk3*-KO in comparison to un-treated KO mice

Long-term potentiation is impaired in *Lmtk3*-KO mice

LTP is a form of synaptic plasticity involving the strengthening of synaptic transmissions after repetitive stimulation. Dysfunctional LTP leads to a number of behavioural abnormalities and cognitive issues (Pittenger, 2013; Stuchlik, 2014). As *Lmtk3*-KO mice display severe cognitive impairments, we performed electrophysiological analysis of the CA1 region of the hippocampus to measure LTP. Theta-burst stimulation of Schaffer collaterals was used to induce LTP and output was recorded by measuring field EPSPs (excitatory post-

synaptic potentials). The recordings revealed that stimulation failed to elicit LTP in *Lmtk3*-KO mice compared to WT mice (Fig. 5A). The average fEPSP slope was significantly lower ($p < 0.01$) in *Lmtk3*-KO mice (111.8 ± 10.09% of baseline) compared to WT (146.8 ± 6.530% of baseline) (Fig. 5B).

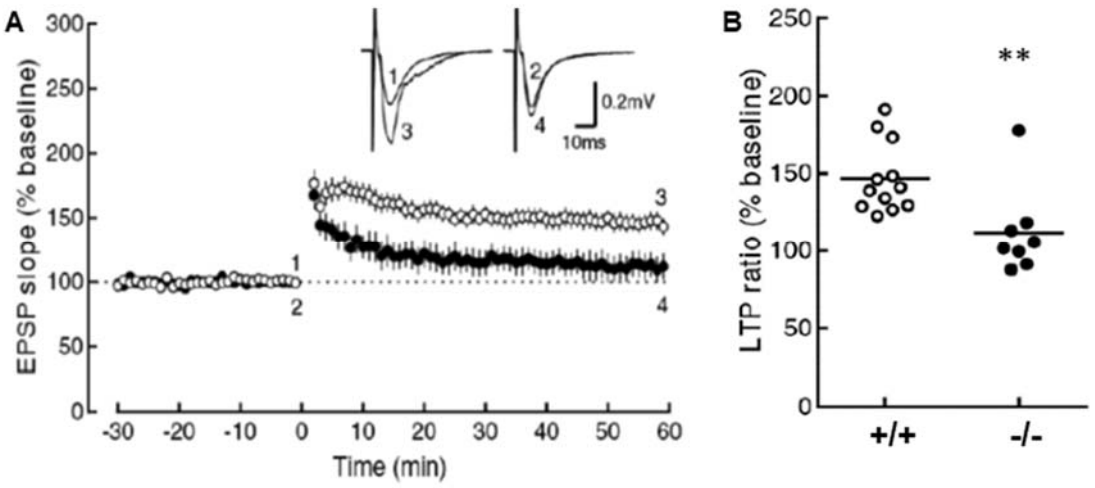

Figure 5. LTP is impaired in *Lmtk3*-KO mice

(A) Time course of LTP induced by theta-burst in WT (open circle) and *Lmtk3*-KO (closed circle). Theta-burst stimulation was applied at time 0 min. Inset: representative traces recorded at times indicated on the graph. (B) LTP calculated as % of the mean EPSP slope recorded from 50 to 60 min after theta-burst stimulation relative to that during the control period. **P < 0.01, un-paired two tailed *t*-test. (WT, $n = 12$; KO, $n = 8$). All values represent means ± SEM.

Loss of LMTK3 leads to abnormal GluA1 trafficking

Trafficking of AMPARs to post-synaptic sites is essential for regulating LTP, and controls memory formation and memory loss (Dong et al., 2015). In addition AMPAR-KO mice, particularly those lacking the GluA1 subunit, exhibit a schizophrenia and schizoaffective phenotype (Barkus et al., 2012; P. J. Fitzgerald et al., 2010). As LTP is impaired in *Lmtk3*-KO mice, we wished to investigate whether changes in AMPAR trafficking could be responsible. After treatment of cultured neurons with AMPA, the definitive agonist for AMPARs, there was less GluA1 on the surface of *Lmtk3*-KO neurons, compared to WT, 15

min post-treatment (Fig. 6A, 6B). No difference in the GluA2 subunit was observed. An 'antibody feeding' immunofluorescence assay also revealed lower levels of surface GluA1 in *Lmtk3*-KO neurons, in addition to increased intracellular GluA1 (Fig. 6C, 6D). As GluA1 trafficking is rapid, we investigated surface and internalized levels of GluA1 at 5, 10, and 15 min post-AMPA treatment. In WT neurons, there is a reduction of GluA1 surface expression 5 min post-treatment, which recovers by 15 min, whereas in *Lmtk3*-KO neurons, there is significantly less change (Fig. 6E, 6F). We found that the loss of surface GluA1 in WT neurons coincided with increased internalized GluA1, and vice versa, as surface GluA1 recovers when internalized GluA1 is reduced 15 min post treatment (Fig. 6G, 6H). This follows the basic model of LTP, where internalization of AMPARs from extra-synaptic sites, followed by transport back to the post-synaptic membrane, occurs in response to stimulation (Anggono & Huganir, 2012; Citri & Malenka, 2008). However, in *Lmtk3*-KO neurons, there is significantly less internalization of surface GluA1, and this internalization occurs at a slower rate. Intracellular GluA1 accumulates after 10 min, which remains 15 min post-treatment, indicating an inability to transport GluA1 to the surface. In accord, surface GluA1 does not recover after 15 min. Total and phosphorylated GluA1 does not change, suggesting that impairment of the endocytic pathway is primarily responsible (Fig. 6I). Previous reports found LMTK3 to be both on the membrane surface and in transferrin-positive endosomes, indicating that it is internalized in the same endocytic pathway as GluA1 (Inoue et al., 2014; Zheng et al., 2015). Co-IP revealed that LMTK3 binds GluA1, leading us to hypothesize that LMTK3 links GluA1 to the endocytic machinery (Fig. 6J).

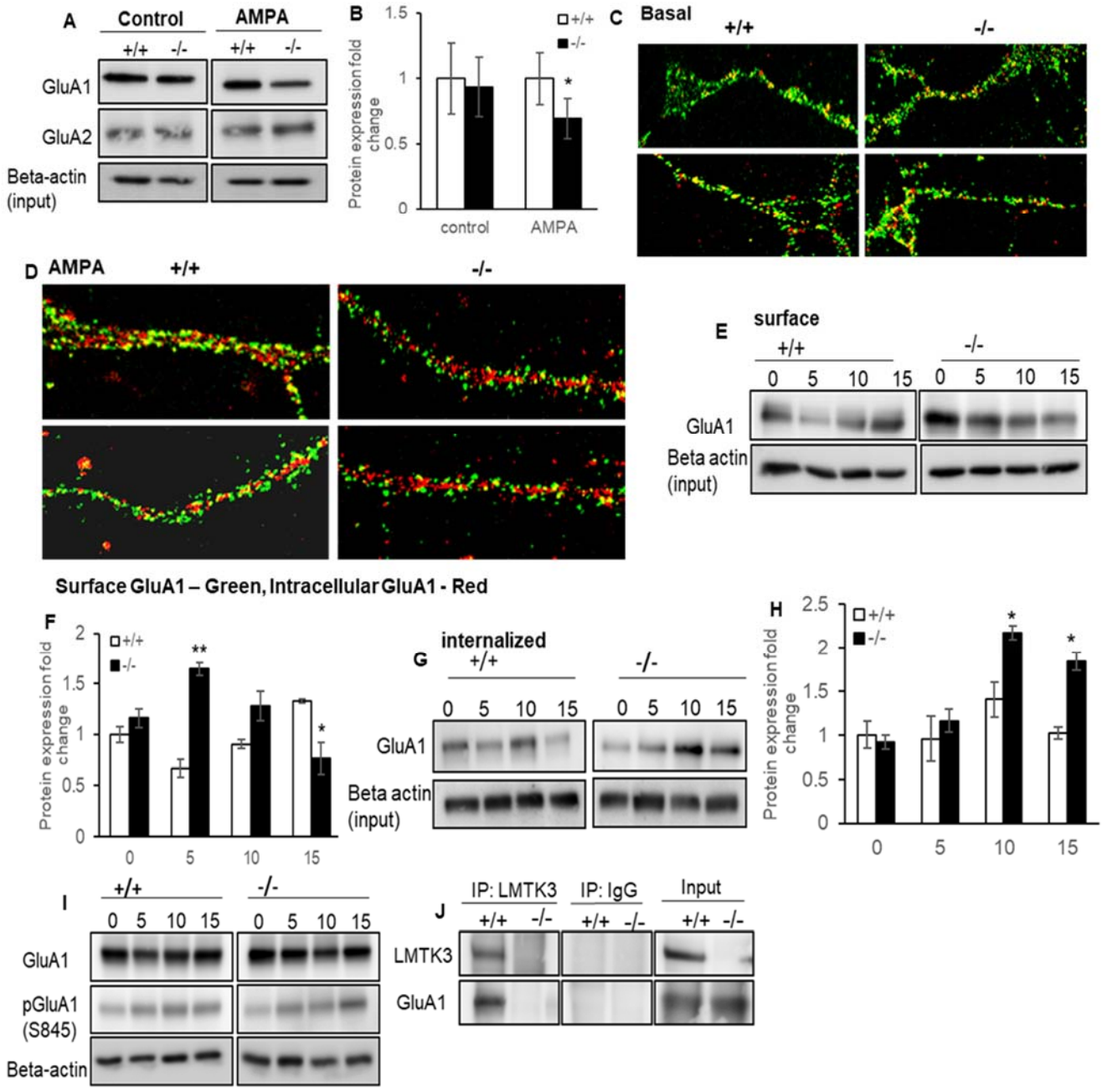

Figure 6. Abnormal GluA1 trafficking in *Lmtk3*-KO neurons

(A-B) Surface biotinylation was performed on cortical and hippocampal neuronal cultures as described in the Methods. (A) Representative immunoblot of surface GluA1 and GluA2 in neurons treated with 100 μM AMPA for 15 min or un-treated (basal), reveals less surface GluA1 in *Lmtk3*-KO neurons after AMPA treatment. No change to GluA2 expression is observed. (B) Quantification of immunoblot as fold change compared to WT. (WT, $n = 4$; KO, $n = 4$).*$P < 0.05$, un-paired two tailed *t*-test . (C-D) Cultured neurons labelled with GluA1 antibody using the 'antibody feeding' method. Neurons were treated with 100 μM AMPA for 15 min or left un-treated (basal). Fluorescent staining reveals GluA1 surface

expression (green) and intracellular expression (red). (C) No difference in GluA1 on the surface or intracellular in un-treated neurons. (D) Surface GluA1 is reduced and intracellular GluA1 is enhanced in *Lmtk3*-KO neurons. (E-F) Changes in GluA1 surface expression after 100 μM AMPA treatment for described times. (E) Surface GluA1 decreases 5 min after treatment and recovers by 15 min in WT neurons. Minimal effect on surface GluA1 is observed in *Lmtk3*-KO neurons. (F) Quantification as fold change compared to WT. (WT, $n = 4$; KO, $n = 4$). *$P < 0.05$, **$P < 0.01$; un-paired two tailed *t*-test. (G-H) Level of internalized GluA1 after 100 μM AMPA treatment for the described times. (G) In WT neurons, GluA1 internalization increases 10 min after AMPA treatment then drops by 15 min. In *Lmtk3*-KO neurons, internalization of GluA1 occurs 10 min after AMPA treatment and remains after 15 min. (H) Quantification as fold change compared to WT. (WT, $n = 4$; KO, $n = 4$). *$P < 0.05$, **$P < 0.01$; un-paired two tailed *t*-test. (I) Total and phosphorylated GluA1 in WT and *Lmtk3*-KO neurons. No significant difference between genotypes. (J) Co-IP using anti-LMTK3 antibody with whole brain lysate reveals that LMTK3 binds GluA1.

Decreased expression of GluA1 in the post-synaptic density of *Lmtk3*-KO mice

An impairment in the transport of GluA1 from an internal pool to the post-synaptic surface should result in a deficit of GluA1 at post-synaptic sites. To investigate this we performed synaptosomal fractionation on forebrain tissue. A significant reduction in the expression of GluA1 within the post-synaptic density of *Lmtk3*-KO mice was discovered (Fig. 7A, 7B). Interestingly, analysis of *Lmtk3*-KO mice treated with clozapine showed that GluA1 expression in the post-synaptic density was equivalent to that of WT mice, 30 min after clozapine injection (Fig. 7C, 7D). The reason for this recovery remains unclear but may explain how clozapine attenuates the behaviour of *Lmtk3*-KO mice.

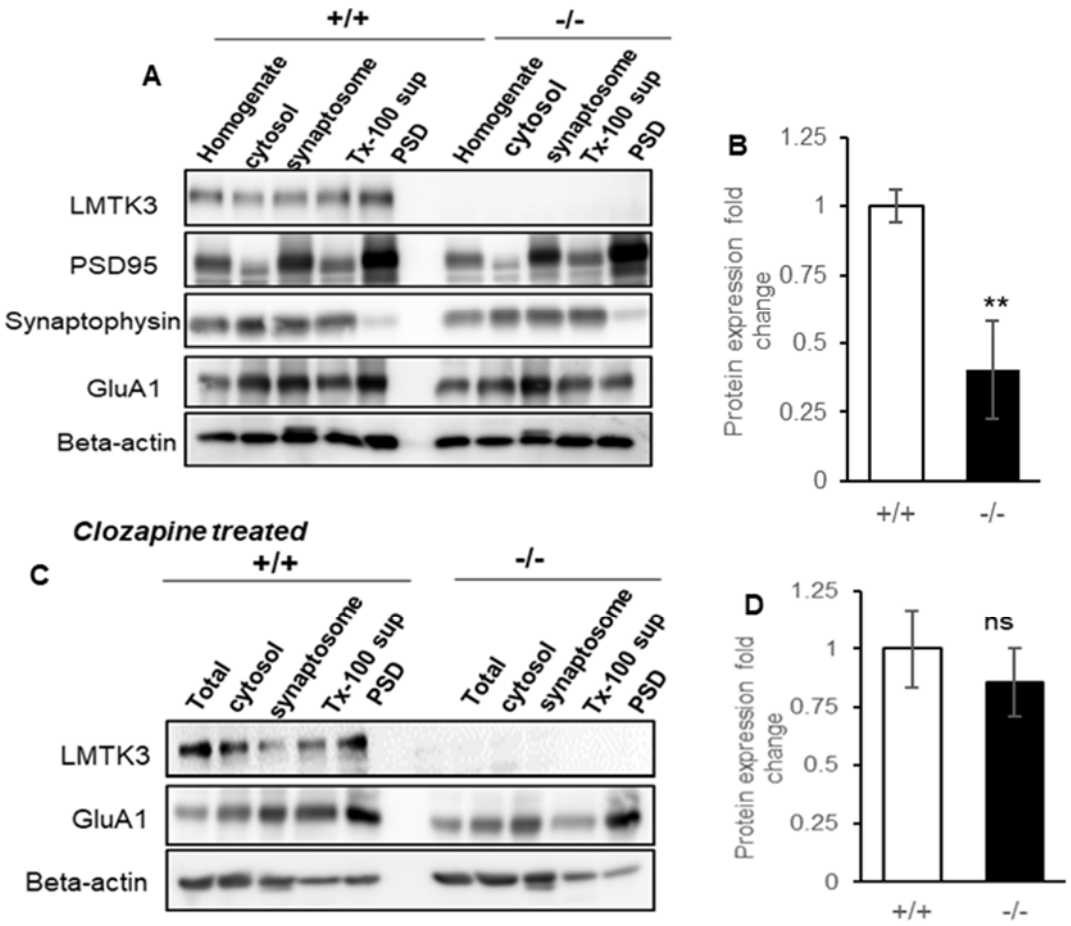

Figure 7. Reduced GluA1 expression in the PSD of *Lmtk3*-KO mice

(A) Synaptosomal fractionation was conducted on forebrain tissue of WT and *Lmtk3*-KO mice as described in Methods ($n = 3$). Representative immunoblot of different fractions probed with PSD95 (post-synaptic marker), synaptophysin (pre-synaptic marker), LMTK3, and GluA1 are shown. The PSD fraction of *Lmtk3*-KO mice shows lower GluA1 levels compared to WT. (B) Quantification as fold change compared to WT. **$P < 0.01$; un-paired two tailed *t*-test. (C) Synaptosomal fractionation of forebrain tissue derived from clozapine-treated mice ($n = 3$). No significant difference in GluA1 expression between genotypes. (D) Quantification as fold change compared to WT. (ns) not significant; un-paired two tailed *t*-test.

Discussion

Modelling human psychiatric disease in animals is challenging, given the objective nature of symptoms and diagnostic tests. Nonetheless, there is a consensus that an effective animal model of mental illness displays phenotypes closely resembling human symptoms and mimic human responses to pharmacological treatment (Chadman et al., 2009). Here we show that *Lmtk3*-KO mice present abnormal behaviour such as deficits in PPI, loss of novelty preference and cognitive dysfunction that are associated with psychiatric disease, primarily schizophrenia and bipolar disorder. Reports have shown that schizophrenia and bipolar disease are closely linked and often overlap (Forstner et al., 2017; Laursen et al., 2009). Hyper-sociability in the three-chamber social interaction test is also displayed, which is surprising, as this is not commonly observed in conjunction with the other abnormal behaviours displayed by *Lmtk3*-KO mice. Though this is the case, there are a number of mouse models with mutations in genes altering AMPAR function which display hyper-sociability similar to that of *Lmtk3*-KO mice (Barkus et al., 2012; Han et al., 2017; Tanda et al., 2009). We hypothesize that the hyper-sociability of *Lmtk3*-KO may be a consequence of abnormal AMPA receptor function. It should also be stated that *Lmtk3*-KO mice show lower levels of depression-like symptoms (Inoue et al., 2014), even though elevated depression is often co-morbid with schizophrenia (Samsom & Wong, 2015). Instead, lower levels of depression can be found in animal models of bipolar disease (Logan & McClung, 2016), highlighting the overlap between schizophrenia and bipolar associated behaviour in *Lmtk3*-KO mice. In addition it has been found that cell specific deletion of GluA1 led to no change in depression-like behaviour of mice, as opposed to global deletion of GluA1 which causes a significant rise (Vogt et al., 2014). Future work should be conducted to analyse the effect of *Lmtk3* depletion on GluA1 within specific regions of the brain and cell types, to determine whether this could play a part in the extreme range of behaviours observed in *Lmtk3*-KO mice.

Lmtk3-KO mice respond well to acute treatment with clozapine, an antipsychotic commonly used to treat schizophrenia and schizoaffective disorders. Clinically, chronic drug treatments are required for efficacy in psychiatric patients, and further investigation is required to determine the effect of chronic administration in *Lmtk3*-KO mice. Our study reveals that *Lmtk3*-KO mice express lower levels of GluA1 in the forebrain, specifically in the post-

synaptic region. Surprisingly, treatment of *Lmtk3*-KO mice with clozapine increased GluA1 expression. The reason for this is still under investigation, hindered by the fact that clozapine's mechanism of action is unclear. A number of studies have shown that clozapine treatment of rodents induces changes in expression of a range of glutamate receptors, including AMPARs, which may account for the upregulated GluA1 in treated *Lmtk3*-KO mice (L. W. Fitzgerald et al., 1995; Meshul et al., 1996).

In *Lmtk3*-KO neurons, we observed reduced trafficking of GluA1 after stimulation with AMPA. As we wished to concentrate on the effect of LMTK3 depletion specifically on AMPA receptors, we did not use standard chemical LTP protocols, bypassing the effect of activating NMDA and other receptors on AMPA trafficking. Our previous report showed that surface expression of GluA1 and GluA2 in cultured neurons, was not affected by the loss of LMTK3; however, these experiments were conducted under basal conditions (Inoue et al., 2014). Trafficking of GluA1 is activity-dependent, and low levels of recycling occurs under basal conditions (Shi et al., 2001). We hypothesize that LMTK3 is involved in the endocytosis and recycling of GluA1, and maybe required to guide early endosomes into the recycling pathway. Consequently, internalized GluA1 accumulates in neurons lacking LMTK3 after AMPA stimulation. Trafficking of GluA2, the other major AMPAR subunit, is not influenced by the loss of LMTK3, which could be due to differences in the activation and trafficking between GluA1 and GluA2. The exact mechanism by which LMTK3 influences GluA1 trafficking is still unknown, but we speculate that it may perform as a scaffold protein between endocytic vesicles and GluA1. This is based on the finding that LMTK3 interacts with both GluA1 and the clathrin-adaptor protein AP2. An interaction between GluA1 and AP2 is necessary for the trafficking of GluA1 (Petrini et al., 2009). Mice lacking expression of GluA1 have been described as a schizophrenia and schizoaffective mouse model and exhibit a range of behaviours similar to that of *Lmtk3*-KO mice (Wiedholz et al., 2008). In addition it has been shown that in the frontal cortex of elderly schizophrenia patients, GluA1 accumulates in early endosomes, due to defects in the recycling pathway (Hammond et al., 2010). *Lmtk3*-KO mice present increased levels of dopamine metabolites in the striatum, yet no changes in the level of dopamine or tyrosine hydroxylase were found, and neither were there changes in the phosphorylation state of DARP32 (Inoue et al., 2014). Therefore, we believe dopamine turnover is indirectly affected by depletion of LMTK3, and does not alter dopaminergic signalling or contribute to the phenotype of *Lmtk3*-KO mice. Although hyperactivity is generally associated with an increase in dopamine, there are examples where

cell-specific changes in GluA1 or treatment with NMDA receptor antagonists can cause hyperactivity independent of dopamine elevation (Chartoff et al., 2005; Inta et al., 2014).

LTP is the most established model of synaptic plasticity, and is characterized by an increase in GluA1 on the post-synaptic surface (Bassani et al., 2013). A pool of recycling endosomes containing GluA1 supply this increase (Park et al., 2004). As GluA1 recycling is impaired in *Lmtk3*-KO neurons, it is reasonable that LTP is severely impaired in *Lmtk3*-KO mice. It is generally accepted that LTP is vital for memory formation and storage (Stuchlik, 2014). Moreover, there are reports that schizophrenia patients, as well as established mouse models of psychiatric disease display disrupted LTP (Balu et al., 2013; Frantseva et al., 2008; Kvajo et al., 2008). We hypothesize that impaired LTP is an important factor in the change of behaviour in *Lmtk3*-KO mice.

To date, only one mutation in LMTK3 has been found in a psychiatric patient, specifically in an autistic child (Iossifov et al., 2012). Autism spectrum disorder (ASD) share phenotypical and genetic similarities with a number of psychiatric diseases including schizophrenia and bipolar disease (Voineagu et al., 2011). Patients diagnosed with ASD often develop psychotic symptoms reminiscent of schizophrenia (Canitano & Pallagrosi, 2017). *Lmtk3* is also recognized as a Fragile X mental retardation protein (FMRP) target (Nebel et al., 2016). FMRP is an RNA binding protein, which regulates a number of neuronal processes including synaptic plasticity. Loss of FMRP leads to Fragile X syndrome which is characterized by severe mental retardation and reports have shown that expression of FMRP and its targets are altered in a number of psychiatric diseases (Fatemi & Folsom, 2011; Fernandez et al., 2013). Little is known about the expression levels of LMTK3 in psychiatric patients, and it would be interesting to see if alterations in LMTK3 levels can be found in patients.

Our data further develops the hypothesis that the glutamatergic system plays a vital role in the maintenance of mental health. It is clear that *Lmtk3*-KO mice display abnormal behaviour, that which commonly associate with psychiatric disease. Therefore, they could be a useful model in the study of behaviour and learning. In addition, *Lmtk3*-KO mice display a human-like response to clozapine, which is ideal for testing the efficacy of new pharmaceuticals. Future work is required to clarify the mechanism by which LMTK3 controls GluA1 trafficking, to further understand the molecular pathways involved in psychiatric disease

Acknowledgements

We thank Naosuke Hoshina for the maintenance of *Lmtk3* mouse line and technical advice, as well as Takanobu Nakazawa and Takeshi Inoue for valuable data discussion. We also thank Steven Douglas Aird for critical reading and editing of this manuscript.

Author contributions: K.M, T.M and T.Y designed the research; K.M and S.K performed the research; K.M and T.Y wrote the paper.

The authors declare no conflict of interest.

References

Anggono, V., & Huganir, R. L. (2012). Regulation of AMPA receptor trafficking and synaptic plasticity. *Curr Opin Neurobiol, 22*(3), 461-469. doi: 10.1016/j.conb.2011.12.006

Balu, D. T., Li, Y., Puhl, M. D., Benneyworth, M. A., Basu, A. C., Takagi, S., . . . Coyle, J. T. (2013). Multiple risk pathways for schizophrenia converge in serine racemase knockout mice, a mouse model of NMDA receptor hypofunction. *Proc Natl Acad Sci U S A, 110*(26), E2400-2409. doi: 10.1073/pnas.1304308110

Barkus, C., Feyder, M., Graybeal, C., Wright, T., Wiedholz, L., Izquierdo, A., . . . Holmes, A. (2012). Do GluA1 knockout mice exhibit behavioral abnormalities relevant to the negative or cognitive symptoms of schizophrenia and schizoaffective disorder? *Neuropharmacology, 62*(3), 1263-1272. doi: 10.1016/j.neuropharm.2011.06.005

Bassani, S., Folci, A., Zapata, J., & Passafaro, M. (2013). AMPAR trafficking in synapse maturation and plasticity. *Cell Mol Life Sci, 70*(23), 4411-4430. doi: 10.1007/s00018-013-1309-1

Becker, A., & Grecksch, G. (2003). Haloperidol and clozapine affect social behaviour in rats postnatally lesioned in the ventral hippocampus. *Pharmacol Biochem Behav, 76*(1), 1-8.

Beherec, L., Lambrey, S., Quilici, G., Rosier, A., Falissard, B., & Guillin, O. (2011). Retrospective review of clozapine in the treatment of patients with autism spectrum disorder and severe disruptive behaviors. *J Clin Psychopharmacol, 31*(3), 341-344. doi: 10.1097/JCP.0b013e318218f4a1

Bongsebandhu-phubhakdi, S., & Manabe, T. (2007). The neuropeptide nociceptin is a synaptically released endogenous inhibitor of hippocampal long-term potentiation. *J Neurosci, 27*(18), 4850-4858. doi: 10.1523/jneurosci.0876-07.2007

Canitano, R., & Pallagrosi, M. (2017). Autism Spectrum Disorders and Schizophrenia Spectrum Disorders: Excitation/Inhibition Imbalance and Developmental Trajectories. *Front Psychiatry, 8*, 69. doi: 10.3389/fpsyt.2017.00069

Chadman, K. K., Yang, M., & Crawley, J. N. (2009). Criteria for validating mouse models of psychiatric diseases. *Am J Med Genet B Neuropsychiatr Genet, 150b*(1), 1-11. doi: 10.1002/ajmg.b.30777

Chartoff, E. H., Heusner, C. L., & Palmiter, R. D. (2005). Dopamine is not required for the hyperlocomotor response to NMDA receptor antagonists. *Neuropsychopharmacology, 30*(7), 1324-1333. doi: 10.1038/sj.npp.1300678

Citri, A., & Malenka, R. C. (2008). Synaptic plasticity: multiple forms, functions, and mechanisms. *Neuropsychopharmacology, 33*(1), 18-41. doi: 10.1038/sj.npp.1301559

Corti, C., Xuereb, J. H., Crepaldi, L., Corsi, M., Michielin, F., & Ferraguti, F. (2011). Altered levels of glutamatergic receptors and Na+/K+ ATPase-alpha1 in the prefrontal cortex of subjects with schizophrenia. *Schizophr Res, 128*(1-3), 7-14. doi: 10.1016/j.schres.2011.01.021

Cosgrove, V. E., Kelsoe, J. R., & Suppes, T. (2016). Toward a Valid Animal Model of Bipolar Disorder: How the Research Domain Criteria Help Bridge the Clinical-Basic Science Divide. *Biol Psychiatry, 79*(1), 62-70. doi: 10.1016/j.biopsych.2015.09.002

Doherty, J. L., & Owen, M. J. (2014). Genomic insights into the overlap between psychiatric disorders: implications for research and clinical practice. *Genome Med, 6*(4), 29. doi: 10.1186/gm546

Dong, Z., Han, H., Li, H., Bai, Y., Wang, W., Tu, M., . . . Wang, Y. T. (2015). Long-term potentiation decay and memory loss are mediated by AMPAR endocytosis. *J Clin Invest, 125*(1), 234-247. doi: 10.1172/jci77888

Du, J., Machado-Vieira, R., & Khairova, R. (2011). Synaptic plasticity in the pathophysiology and treatment of bipolar disorder. *Curr Top Behav Neurosci, 5*, 167-185. doi: 10.1007/7854_2010_65

Fatemi, S. H., & Folsom, T. D. (2011). The role of fragile X mental retardation protein in major mental disorders. *Neuropharmacology, 60*(7-8), 1221-1226. doi: 10.1016/j.neuropharm.2010.11.011

Fehr, B. S., Ozcan, M. E., & Suppes, T. (2005). Low doses of clozapine may stabilize treatment-resistant bipolar patients. *Eur Arch Psychiatry Clin Neurosci, 255*(1), 10-14. doi: 10.1007/s00406-004-0528-8

Fernandez, E., Rajan, N., & Bagni, C. (2013). The FMRP regulon: from targets to disease convergence. *Front Neurosci, 7*, 191. doi: 10.3389/fnins.2013.00191

Fitzgerald, L. W., Deutch, A. Y., Gasic, G., Heinemann, S. F., & Nestler, E. J. (1995). Regulation of cortical and subcortical glutamate receptor subunit expression by antipsychotic drugs. *J Neurosci, 15*(3 Pt 2), 2453-2461.

Fitzgerald, P. J., Barkus, C., Feyder, M., Wiedholz, L. M., Chen, Y. C., Karlsson, R. M., . . . Holmes, A. (2010). Does gene deletion of AMPA GluA1 phenocopy features of schizoaffective disorder? *Neurobiol Dis, 40*(3), 608-621. doi: 10.1016/j.nbd.2010.08.005

Forero, D. A., Arboleda, G. H., Vasquez, R., & Arboleda, H. (2009). Candidate genes involved in neural plasticity and the risk for attention-deficit hyperactivity disorder: a meta-analysis of 8 common variants. *J Psychiatry Neurosci, 34*(5), 361-366.

Forstner, A. J., Hecker, J., Hofmann, A., & Maaser, A. (2017). Identification of shared risk loci and pathways for bipolar disorder and schizophrenia. *12*(2), e0171595. doi: 10.1371/journal.pone.0171595

Frantseva, M. V., Fitzgerald, P. B., Chen, R., Moller, B., Daigle, M., & Daskalakis, Z. J. (2008). Evidence for impaired long-term potentiation in schizophrenia and its relationship to motor skill learning. *Cereb Cortex, 18*(5), 990-996. doi: 10.1093/cercor/bhm151

Frye, M. A., Ketter, T. A., Altshuler, L. L., Denicoff, K., Dunn, R. T., Kimbrell, T. A., . . . Post, R. M. (1998). Clozapine in bipolar disorder: treatment implications for other atypical antipsychotics. *J Affect Disord, 48*(2-3), 91-104.

Gandal, M. J. (2018). Shared molecular neuropathology across major psychiatric disorders parallels polygenic overlap. *359*(6376), 693-697. doi: 10.1126/science.aad6469

Gray, L., van den Buuse, M., Scarr, E., Dean, B., & Hannan, A. J. (2009). Clozapine reverses schizophrenia-related behaviours in the metabotropic glutamate receptor 5 knockout mouse: association with N-methyl-D-aspartic acid receptor up-regulation. *Int J Neuropsychopharmacol, 12*(1), 45-60. doi: 10.1017/s1461145708009085

Hammond, J. C., McCullumsmith, R. E., Funk, A. J., Haroutunian, V., & Meador-Woodruff, J. H. (2010). Evidence for abnormal forward trafficking of AMPA receptors in frontal cortex of elderly patients with schizophrenia. *Neuropsychopharmacology, 35*(10), 2110-2119. doi: 10.1038/npp.2010.87

Han, M., Mejias, R., Chiu, S. L., Rose, R., Adamczyk, A., Huganir, R., & Wang, T. (2017). Mice lacking GRIP1/2 show increased social interactions and enhanced phosphorylation at GluA2-S880. *Behav Brain Res, 321*, 176-184. doi: 10.1016/j.bbr.2016.12.042

Heckers, S., & Konradi, C. (2002). Hippocampal neurons in schizophrenia. *J Neural Transm (Vienna), 109*(5-6), 891-905. doi: 10.1007/s007020200073

Henley, J. M., & Wilkinson, K. A. (2013). AMPA receptor trafficking and the mechanisms underlying synaptic plasticity and cognitive aging. *Dialogues Clin Neurosci, 15*(1), 11-27.

Huganir, R. L., & Nicoll, R. A. (2013). AMPARs and synaptic plasticity: the last 25 years. *Neuron, 80*(3), 704-717. doi: 10.1016/j.neuron.2013.10.025

Inoue, T., Hoshina, N., Nakazawa, T., Kiyama, Y., Kobayashi, S., Abe, T., . . . Yamamoto, T. (2014). LMTK3 deficiency causes pronounced locomotor hyperactivity and impairs endocytic trafficking. *J Neurosci, 34*(17), 5927-5937. doi: 10.1523/jneurosci.1621-13.2014

Inoue, T., Kon, T., Ohkura, R., Yamakawa, H., Ohara, O., Yokota, J., & Sutoh, K. (2008). BREK/LMTK2 is a myosin VI-binding protein involved in endosomal membrane trafficking. *Genes Cells, 13*(5), 483-495. doi: 10.1111/j.1365-2443.2008.01184.x

Inta, D., Vogt, M. A., Elkin, H., Weber, T., Lima-Ojeda, J. M., Schneider, M., . . . Gass, P. (2014). Phenotype of mice with inducible ablation of GluA1 AMPA receptors during late adolescence: relevance for mental disorders. *Hippocampus, 24*(4), 424-435. doi: 10.1002/hipo.22236

Iossifov, I., Ronemus, M., Levy, D., Wang, Z., Hakker, I., Rosenbaum, J., . . . Wigler, M. (2012). De novo gene disruptions in children on the autistic spectrum. *Neuron, 74*(2), 285-299. doi: 10.1016/j.neuron.2012.04.009

Jones, C. A., Watson, D. J., & Fone, K. C. (2011). Animal models of schizophrenia. *Br J Pharmacol, 164*(4), 1162-1194. doi: 10.1111/j.1476-5381.2011.01386.x

Jun, C., Choi, Y., Lim, S. M., Bae, S., Hong, Y. S., Kim, J. E., & Lyoo, I. K. (2014). Disturbance of the glutamatergic system in mood disorders. *Exp Neurobiol, 23*(1), 28-35. doi: 10.5607/en.2014.23.1.28

Konradi, C., & Heckers, S. (2003). Molecular aspects of glutamate dysregulation: implications for schizophrenia and its treatment. *Pharmacol Ther, 97*(2), 153-179.

Kvajo, M., McKellar, H., Arguello, P. A., Drew, L. J., Moore, H., MacDermott, A. B., . . . Gogos, J. A. (2008). A mutation in mouse Disc1 that models a schizophrenia risk allele leads to specific alterations in neuronal architecture and cognition. *Proc Natl Acad Sci U S A, 105*(19), 7076-7081. doi: 10.1073/pnas.0802615105

Laursen, T. M., Agerbo, E., & Pedersen, C. B. (2009). Bipolar disorder, schizoaffective disorder, and schizophrenia overlap: a new comorbidity index. *J Clin Psychiatry, 70*(10), 1432-1438. doi: 10.4088/JCP.08m04807

Leo, D., & Gainetdinov, R. R. (2013). Transgenic mouse models for ADHD. *Cell Tissue Res, 354*(1), 259-271. doi: 10.1007/s00441-013-1639-1

Li, X. B., Tang, Y. L., Wang, C. Y., & de Leon, J. (2015). Clozapine for treatment-resistant bipolar disorder: a systematic review. *Bipolar Disord, 17*(3), 235-247. doi: 10.1111/bdi.12272

Lin, J. W., Ju, W., Foster, K., Lee, S. H., Ahmadian, G., Wyszynski, M., . . . Sheng, M. (2000). Distinct molecular mechanisms and divergent endocytotic pathways of AMPA receptor internalization. *Nat Neurosci, 3*(12), 1282-1290. doi: 10.1038/81814

Logan, R. W., & McClung, C. A. (2016). Animal models of bipolar mania: The past, present and future. *Neuroscience, 321*, 163-188. doi: 10.1016/j.neuroscience.2015.08.041

McOmish, C. E., Lira, A., Hanks, J. B., & Gingrich, J. A. (2012). Clozapine-induced locomotor suppression is mediated by 5-HT2A receptors in the forebrain. *Neuropsychopharmacology, 37*(13), 2747-2755. doi: 10.1038/npp.2012.139

Meador-Woodruff, J. H., Hogg, A. J., Jr., & Smith, R. E. (2001). Striatal ionotropic glutamate receptor expression in schizophrenia, bipolar disorder, and major depressive disorder. *Brain Res Bull, 55*(5), 631-640.

Meshul, C. K., Bunker, G. L., Mason, J. N., Allen, C., & Janowsky, A. (1996). Effects of subchronic clozapine and haloperidol on striatal glutamatergic synapses. *J Neurochem, 67*(5), 1965-1973.

Nebel, R. A., Zhao, D., Pedrosa, E., Kirschen, J., Lachman, H. M., Zheng, D., & Abrahams, B. S. (2016). Reduced CYFIP1 in Human Neural Progenitors Results in Dysregulation of Schizophrenia and Epilepsy Gene Networks. *PLoS One, 11*(1), e0148039. doi: 10.1371/journal.pone.0148039

Park, M., Penick, E. C., Edwards, J. G., Kauer, J. A., & Ehlers, M. D. (2004). Recycling endosomes supply AMPA receptors for LTP. *Science, 305*(5692), 1972-1975. doi: 10.1126/science.1102026

Petrini, E. M., Lu, J., Cognet, L., Lounis, B., Ehlers, M. D., & Choquet, D. (2009). Endocytic trafficking and recycling maintain a pool of mobile surface AMPA receptors required for synaptic potentiation. *Neuron, 63*(1), 92-105. doi: 10.1016/j.neuron.2009.05.025

Pittenger, C. (2013). Disorders of memory and plasticity in psychiatric disease. *Dialogues Clin Neurosci, 15*(4), 455-463.

Qiao, H., Noda, Y., Kamei, H., Nagai, T., Furukawa, H., Miura, H., . . . Nabeshima, T. (2001). Clozapine, but not haloperidol, reverses social behavior deficit in mice during withdrawal from chronic phencyclidine treatment. *Neuroreport, 12*(1), 11-15.

Remington, G., Lee, J., Agid, O., Takeuchi, H., Foussias, G., Hahn, M., . . . Powell, V. (2016). Clozapine's critical role in treatment resistant schizophrenia: ensuring both safety and use. *Expert Opin Drug Saf, 15*(9), 1193-1203. doi: 10.1080/14740338.2016.1191468

Rotharmel, M., Szymoniak, F., Pollet, C., Beherec, L., Quesada, P., Leclerc, S., . . . Guillin, O. (2018). Eleven Years of Clozapine Experience in Autism Spectrum Disorder: Efficacy and Tolerance. *J Clin Psychopharmacol, 38*(6), 577-581. doi: 10.1097/jcp.0000000000000955

Rubio, M. D., Drummond, J. B., & Meador-Woodruff, J. H. (2012). Glutamate receptor abnormalities in schizophrenia: implications for innovative treatments. *Biomol Ther (Seoul), 20*(1), 1-18. doi: 10.4062/biomolther.2012.20.1.001

Samsom, J. N., & Wong, A. H. (2015). Schizophrenia and Depression Co-Morbidity: What We have Learned from Animal Models. *Front Psychiatry, 6*, 13. doi: 10.3389/fpsyt.2015.00013

Sandner, G., & Canal, N. M. (2007). Relationship between PPI and baseline startle response. *Cogn Neurodyn, 1*(1), 27-37. doi: 10.1007/s11571-006-9008-3

Shi, S., Hayashi, Y., Esteban, J. A., & Malinow, R. (2001). Subunit-specific rules governing AMPA receptor trafficking to synapses in hippocampal pyramidal neurons. *Cell, 105*(3), 331-343.

Shoji, H., & Miyakawa, T. (2018). Relationships between the acoustic startle response and prepulse inhibition in C57BL/6J mice: a large-scale meta-analytic study. *11*(1), 42. doi: 10.1186/s13041-018-0382-7

Siskind, D., McCartney, L., Goldschlager, R., & Kisely, S. (2016). Clozapine v. first- and second-generation antipsychotics in treatment-refractory schizophrenia: systematic

review and meta-analysis. *Br J Psychiatry, 209*(5), 385-392. doi: 10.1192/bjp.bp.115.177261

Stephan, K. E., Baldeweg, T., & Friston, K. J. (2006). Synaptic plasticity and dysconnection in schizophrenia. *Biol Psychiatry, 59*(10), 929-939. doi: 10.1016/j.biopsych.2005.10.005

Stuchlik, A. (2014). Dynamic learning and memory, synaptic plasticity and neurogenesis: an update. *Front Behav Neurosci, 8*, 106. doi: 10.3389/fnbeh.2014.00106

Swerdlow, N. R., & Geyer, M. A. (1993). Clozapine and haloperidol in an animal model of sensorimotor gating deficits in schizophrenia. *Pharmacol Biochem Behav, 44*(3), 741-744.

Takano, T., Tomomura, M., Yoshioka, N., Tsutsumi, K., Terasawa, Y., Saito, T., . . . Hisanaga, S. (2012). LMTK1/AATYK1 is a novel regulator of axonal outgrowth that acts via Rab11 in a Cdk5-dependent manner. *J Neurosci, 32*(19), 6587-6599. doi: 10.1523/jneurosci.5317-11.2012

Takano, T., Urushibara, T., Yoshioka, N., Saito, T., Fukuda, M., Tomomura, M., & Hisanaga, S. (2014). LMTK1 regulates dendritic formation by regulating movement of Rab11A-positive endosomes. *Mol Biol Cell, 25*(11), 1755-1768. doi: 10.1091/mbc.E14-01-0675

Tanda, K., Nishi, A., Matsuo, N., Nakanishi, K., Yamasaki, N., Sugimoto, T., . . . Miyakawa, T. (2009). Abnormal social behavior, hyperactivity, impaired remote spatial memory, and increased D1-mediated dopaminergic signaling in neuronal nitric oxide synthase knockout mice. *Mol Brain, 2*, 19. doi: 10.1186/1756-6606-2-19

Vogt, M. A., Elkin, H., Pfeiffer, N., Sprengel, R., Gass, P., & Inta, D. (2014). Impact of adolescent GluA1 AMPA receptor ablation in forebrain excitatory neurons on behavioural correlates of mood disorders. *Eur Arch Psychiatry Clin Neurosci, 264*(7), 625-629. doi: 10.1007/s00406-014-0509-5

Voineagu, I., Wang, X., Johnston, P., Lowe, J. K., Tian, Y., Horvath, S., . . . Geschwind, D. H. (2011). Transcriptomic analysis of autistic brain reveals convergent molecular pathology. *Nature, 474*(7351), 380-384. doi: 10.1038/nature10110

Wiedholz, L. M., Owens, W. A., Horton, R. E., Feyder, M., Karlsson, R. M., Hefner, K., . . . Holmes, A. (2008). Mice lacking the AMPA GluR1 receptor exhibit striatal hyperdopaminergia and 'schizophrenia-related' behaviors. *Mol Psychiatry, 13*(6), 631-640. doi: 10.1038/sj.mp.4002056

Zheng, N., Jeyifous, O., Munro, C., Montgomery, J. M., & Green, W. N. (2015). Synaptic activity regulates AMPA receptor trafficking through different recycling pathways. *Elife, 4*. doi: 10.7554/eLife.06878